Immunity
Article

B Cell-Specific Deletion of Protein-Tyrosine Phosphatase Shp1 Promotes B-1a Cell Development and Causes Systemic Autoimmunity

Lily I. Pao,[1,*] Kong-Peng Lam,[2] Joel M. Henderson,[3] Jeffery L. Kutok,[3] Marat Alimzhanov,[4] Lars Nitschke,[5] Matthew L. Thomas,[6,7] Benjamin G. Neel,[1] and Klaus Rajewsky[4,*]
[1] Cancer Biology Program, Division of Hematology/Oncology, Department of Medicine, Beth Israel Deaconess Medical Center, Boston, MA 02115, USA
[2] Laboratory of Molecular and Cellular Immunology, Biomedical Sciences Institutes, Agency for Science, Technology and Research and Singapore Immunology Network, Proteos, Singapore 138673, Singapore
[3] Department of Pathology, Brigham and Women's Hospital, Boston, MA 02115, USA
[4] The CBR Institute for Biomedical Research, Harvard Medical School, Boston, MA 02115, USA
[5] Department of Genetics, University of Erlangen, 91058 Erlangen, Germany
[6] Howard Hughes Medical Institute and Department of Pathology, Washington University School of Medicine, St. Louis, MO 63110, USA
[7] This author died during the early stages of this work.
*Correspondence: lpao@bidmc.harvard.edu (L.I.P.), rajewsky@cbr.med.harvard.edu (K.R.)
DOI 10.1016/j.immuni.2007.04.016

SUMMARY

Spontaneous loss-of-function mutations in the protein-tyrosine phosphatase Shp1 cause the motheaten phenotype, characterized by widespread inflammation and autoimmunity. Because Shp1 is expressed in all hematopoietic cells, it has been unclear which aspects of the motheaten phenotypes are primary effects of Shp1 deficiency. We generated mice (*Ptpn6*$^{f/f}$;CD19-*cre*) that delete Shp1 specifically in B cells. Analysis of these mice indicates that the increase in B-1a cells in *motheaten* mice is a cell-autonomous consequence of Shp1 deficiency. Shp1-deficient B-1a cells could be derived from adult bone marrow and had N-nucleotide additions, consistent with an adult origin. Shp1 deficiency altered calcium response evoked by B cell antigen receptors and impaired CD40-evoked proliferation. Young *Ptpn6*$^{f/f}$;CD19-*cre* mice exhibited elevated serum immunoglobulins and impaired antibody responses to immunization, whereas older *Ptpn6*$^{f/f}$;CD19-*cre* mice developed systemic autoimmunity, characterized by DNA antibodies and immune complex glomerulonephritis. Thus, Shp1 deficiency in B cells alone perturbs B cell development and causes autoimmune disease.

INTRODUCTION

B lymphoid progenitors undergo several differentiation steps in the bone marrow (BM), including rearrangement of their immunoglobulin (Ig) loci, leading to expression of B cell antigen receptors (BCRs) on their cell surface. They then migrate to the spleen as BCR$^+$ transitional B cells, and in the spleen they mature into full-fledged follicular "B-2" cells. Although B-2 cells predominate, other B cell subsets, including marginal zone (MZ) B cells and "B-1" cells, also reside in the spleen. Although rare in the spleen, B-1 cells comprise a substantial fraction of B cells in the peritoneal and pleural cavities and are believed to contribute primarily to T independent responses (Berland and Wortis, 2002).

B-1 cell ontogeny remains controversial, with two general models proposed. The "lineage model" holds that B-1 and B-2 cells are derived from two developmentally defined cell lineages, with persistent B-1a cells in adult animals because of their ability to self-renew (Kantor and Herzenberg, 1993). Support for this model is provided by transplantation experiments in which fetal and neonatal liver or omentum gives rise to CD5$^+$ B-1 (B-1a) cells, whereas adult BM yields B-2 cells. The recent identification of lineage (Lin)$^-$B220$^-$CD19$^+$AA4.1$^+$ cells in adult BM, which have a propensity to generate B-1 cells, lends support to the idea that B-1 cells are derived from a distinct cell lineage (Montecino-Rodriguez et al., 2006). The alternative "induced-differentiation" model proposes that B-1a cells derive from B-2 cells exposed to strong BCR signals (Berland and Wortis, 2002; Haughton et al., 1993). Consistent with this model, BCR cross-linking in the presence of appropriate stimuli (e.g., interleukin-6) induces splenic B-2 cells to express CD5 and acquire other B-1a cell features, including phorbol ester responsiveness and downregulation of CD23 and IgD (Berland and Wortis, 2002). Studies of genetically manipulated mice indicate that the strength of BCR signaling may control the development, persistence, or both of B-1a and B-2 cells. Mutations that impair BCR signal strength (e.g., Rho-family GTP-GDP exchange factor Vav or

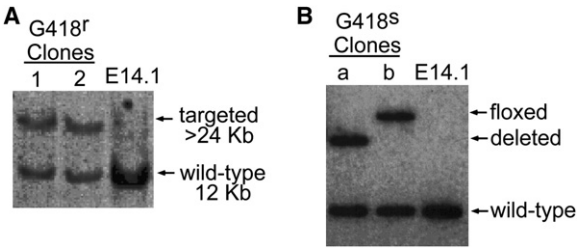

Figure 1. Generation of a Conditional *Ptpn6* Allele

(A) Southern blot of SpeI-digested genomic DNA from two G418-resistant (G418^r) clones and wild-type ES cells, hybridized with the probe in (Figure S1).

(B) Southern blot of SpeI-digested genomic DNA from wild-type ES cells and two G418-sensitive (G418^s) clones, hybridized with the same probe.

phospholipase PLCγ2 deletion) result in reduced B-1a and B-2 cells, whereas mutations that enhance BCR signaling (e.g., CD22 or protein tyrosine kinase Lyn deletion), expand the B-1a population (Berland and Wortis, 2002; Casola et al., 2004).

The mouse mutant, *motheaten* (*me*/*me*), and its allelic variant, *viable motheaten* (*me^v*/*me^v*), carry mutations in the gene *Ptpn6*, which encodes the protein-tyrosine phosphatase Shp1 (Shultz et al., 1993; Tsui et al., 1993). Whereas *me*/*me* mice lack Shp1 protein, *me^v*/*me^v* mice express aberrantly spliced Shp1 variants that retain ~20% catalytic activity (Kozolowski et al., 1993). Shp1 is expressed in hematopoietic cells and plays a signal-attenuating role in pathways initiated by many growth factors, cytokines, and immunoreceptor tyrosine-based activation motif (ITAM)-containing receptors (Neel et al., 2003). Consequently, *me*/*me* and *me^v*/*me^v* mice exhibit multiple hematologic, inflammatory, and autoimmune defects. The key phenotypic features, including retarded growth, alopecia, and inflamed paws, manifest within 1–2 weeks after birth, and the mice die from interstitial pneumonitis within 12 weeks of age. During their short lives, these mice develop enlarged spleens and lymph nodes, containing large numbers of myeloid cells, plasma cells, and Mott cells. The myeloid cell infiltrates in the skin, liver, muscles, and lung are likely to cause tissue damage (Shultz, 1998). Although *me*/*me* mice have a shorter life span than *me^v*/*me^v* mice, their overall phenotype is similar; hence, we hereafter refer generically to "*motheaten* mice" and the "motheaten phenotype," respectively.

Although the development of inflammation and their early demise do not require B and T cells, *motheaten* mice have multiple lymphoid abnormalities, including hypergammaglobulinaemia with circulating autoantibodies and immune-complex deposition in the thymus, lungs, and kidneys (Shultz, 1998). Although the absolute number of splenic B cells is normal, *motheaten* mice have an increased percentage of splenic B-1a cells, suggesting that Shp1 deficiency causes expansion of B-1a cells at the expense of B-2 cells. Consistent with the reduced number of B-2 cells, BM B cell development is severely impaired in *motheaten* mice. Given the widespread inflammation and myeloid expansion in *motheaten* mice, it has been difficult to define which lymphoid defects are cell autonomous; indeed, early studies suggested that at least some B cell abnormalities in these mice are caused by aberrant myeloid cells (Hayashi et al., 1988; Medlock et al., 1987). Whether B-1a cell expansion and autoimmunity in *motheaten* mice are B cell-autonomous effects of Shp1 deficiency remain unclear.

Cyster and Goodnow attempted to address these issues by reconstituting mice with a mixture of wild-type (WT) and *motheaten* BM. The resultant chimeras lacked obvious inflammatory lesions (Cyster and Goodnow, 1995), and the *motheaten*-derived B cells in these chimeras had a B-2 phenotype, increased BCR-evoked calcium flux, and a reduced signaling threshold for self-antigen. Nevertheless, *motheaten*-derived myeloid cells may have influenced B cell development in these chimeras even in the absence of overt inflammatory disease. Also, because this study used Ig-transgenic mice that dictate development of B-2 cells, the effect of Shp1 deficiency on B-1 versus B-2 cell development remained unclear. To define the B cell-autonomous effects of Shp1 deficiency unambiguously, we analyzed mice lacking Shp1 expression only in B cells.

RESULTS

Generation of a Conditional *Ptpn6* Allele

The murine *Ptpn6* gene has two alternative first exons, exon 1(I), expressed primarily in epithelial cells and 1(II), found in hematopoietic cells (Martin et al., 1999). We generated a targeting vector (Figure S1 in the Supplemental Data available online) to conditionally delete exons 1(II)–9, electroporated ES cells, and identified homologous recombinants by Southern blotting (Figure 1A). Two such clones were transiently transfected with a Cre-encoding plasmid to excise the *loxP*-flanked (floxed) neomycin resistance cassette (*neo^r*). Two clones with an appropriately floxed (f) locus were used to generate chimeras (Figure 1B), which were bred to C57BL/6 mice to obtain germline transmission of the floxed allele.

Mice homozygous for floxed *Ptpn6* (*Ptpn6$^{f/f}$*) were normal, indicating that the inserted *loxP* sites did not perturb Shp1 expression. *Ptpn6$^{f/f}$* mice were crossed to mice that carried the *Mx1-cre* transgene, and that expressed Cre recombinase widely, including in hematopoietic cells, in response to type I interferon (IFN) (Kühn et al., 1995). *Ptpn6$^{f/f}$* neonates with or without the *Mx1-cre* transgene were injected with a single dose of IFNα. Only those with the *Mx1-cre* transgene developed the motheaten phenotype (data not shown), confirming that deletion of *Ptpn6* exons 1(II)–9 is sufficient to induce the motheaten phenotype and indicating that floxed *Ptpn6* mice can be used to dissect the cell-type-specific functions of Shp1.

Shp1 Deficiency in B Cells Promotes B-1a Cell Differentiation

To assess the effects of Shp1 deficiency in B lymphocytes, we crossed *Ptpn6$^{f/f}$* with CD19-*cre* mice (Rickert

et al., 1997). Splenic, peritoneal, and BM-derived macrophages from 4- to 8-month-old *Ptpn6*$^{f/f}$;CD19-*cre* mice showed no evidence of Shp1 deletion (Figure S2; data not shown), consistent with studies of CD19-*cre* mice crossed to floxed enhanced yellow fluorescent protein (eYFP) reporter mice (Ye et al., 2003). Thus, CD19-*cre* expression appears to promote floxed *Ptpn6* excision specifically in B cells.

Consistent with earlier reports that B cells are dispensable for the development of the inflammatory disease in *motheaten* mice, *Ptpn6*$^{f/f}$;CD19-*cre* mice exhibited no overt abnormalities (Shultz, 1998). The absolute numbers of splenocytes (Figure 2A) and splenic CD19$^+$ B cells (Figures 2B and 2C) were similar in 11- to 12-week-old control *Ptpn6*$^{+/+}$;CD19-*cre* and mutant *Ptpn6*$^{f/f}$;CD19-*cre* mice. However, splenic B cells in mutant mice expressed elevated amounts of CD19 (Figure 2D). Also, in sharp contrast to normal splenic B cells, most IgM$^+$ splenic B cells in mutant mice expressed low amounts of surface CD5 and B220, reminiscent of B-1a cells (Figures 2B and 2C). Despite their reduced B220 expression, these splenic B cells expressed large amounts of CD45, indicating switching of B220 to other isoforms (Figure 2D). Consistent with the B-1a phenotype, surface IgD expression also was decreased in Shp1-deficient splenic B cells in mutant mice. However, unlike the IgM^{hi} phenotype associated with normal B-1a cells, surface IgM was reduced in Shp1-deficient splenic B cells (Figure 2D). CD43 is normally expressed by a fraction of IgM$^+$CD5$^+$ splenic B-1a cells (Figure S3A), and the percentage and absolute number of CD43$^+$IgM$^+$CD5$^+$ cells were increased in the spleens of mutant mice (Figure S3B). There was also a substantial expansion of CD43$^+$ cells within the splenic IgM$^+$CD5$^-$ population (Figures S3A and S3B). These CD43$^+$IgM$^+$CD5$^-$ cells may represent B-1b cells, suggesting that Shp1 deficiency affects this population as well.

Closer examination of the splenic B cell subsets in *Ptpn6*$^{f/f}$;CD19-*cre* mice revealed a clear reduction in CD23$^+$CD21$^+$IgM$^+$ follicular (FO) B cells and CD21^{hi}IgM^{hi}CD1d^{hi} MZ B cells because the majority of IgM$^+$ B cells were CD23$^-$ and CD21$^-$ (Figures 2E and 2G, data not shown). Although AA4.1$^+$B220^{hi} transitional (Tr) B cells were present, they too were reduced in *Ptpn6*$^{f/f}$;CD19-*cre* spleens (Figures 2F and 2G). Within the Tr B compartment, the proportions of the T1 (IgM$^+$CD23$^-$), T2 (IgM$^+$CD23$^+$), and T3 (IgM^{lo}CD23$^+$) subsets were decreased, with most AA4.1$^+$B220^{hi} B cells being IgM^{lo}CD23$^-$. Thus, deletion of *Ptpn6* in developing B cells has a profound effect on B cell differentiation, resulting in splenic B cells that predominantly express surface markers characteristic of B-1a cells (Hardy and Hayakawa, 2001).

We asked whether the persistent B-2 cells in the spleens of *Ptpn6*$^{f/f}$;CD19-*cre* mice had failed to delete Shp1. IgM$^+$ B cells from control (*Ptpn6*$^{f/+}$;CD19-*cre* or *Ptpn6*$^{f/f}$) or mutant mice were collected by FACS on the basis of their CD5 expression and analyzed by Southern blotting and immunoblotting. *Ptpn6*-gene deletion was efficient in both the CD5$^+$ and CD5$^-$ populations (Figure 2H), but some Shp1 protein was detectable in the CD5$^-$ fraction (Figure 2I). This correlation between CD5 expression and the absence of Shp1 protein suggests that developing B cells in *Ptpn6*$^{f/f}$;CD19-*cre* mice may acquire the B-1a phenotype as their Shp1-protein amounts decrease.

As in the spleen, the percentage of IgM$^+$ B cells that were CD5$^+$ and B220^{lo} was increased in the lymph nodes of *Ptpn6*$^{f/f}$;CD19-*cre* mice (Figures 3A and 3B). Interestingly, the number of CD19$^+$ B cells was significantly reduced, reflecting a 4-fold decrease in IgM$^+$CD5$^-$ B-2 cells, concomitant with a 3-fold increase in IgM$^+$CD5$^+$ B cells (Figure 3B, $p < 0.0005$). By contrast, Shp1 deficiency in B cells significantly increased the total number of peritoneal cells (Figure 2A, $p < 0.05$) because of a 5-fold increase in CD19$^+$ B cells (Figures 3C and 3D). Approximately 90% of IgM$^+$ peritoneal B cells were CD5$^+$ and B220^{lo}. The distinct effects of Shp1 deficiency on B cell numbers at various anatomical locations presumably reflect the relative ability of wild-type and Shp1-deficient B cells to home, survive, or expand in different sites.

Typically, B-1a cells are absent in normal BM. However, we readily detected IgM$^+$CD5$^+$ B cells in BM from *Ptpn6*$^{f/f}$;CD19-*cre* mice (Figures 3E and 3F). The BM B220^{hi}IgM$^+$ (fraction F) was significant reduced, whereas other fractions remained normal (Figure S4). Because CD19-*cre* mediated excision is incomplete in BM B lymphoid precursors, it remains unclear whether the IgM$^+$CD5$^+$ B cells in the BM of *Ptpn6*$^{f/f}$;CD19-*cre* mice are recirculating, mature B cells or newly generated B cells that acquire the B-1a phenotype as their Shp1-protein amounts decline.

Adult Origin of B-1a Cells in *Ptpn6*$^{f/f}$;CD19-*cre* Mice

To investigate the origin of B-1a cells in *Ptpn6*$^{f/f}$;CD19-*cre* mice, we transferred BM cells from adult Ly5.2$^+$ *Ptpn6*$^{f/f}$;CD19-*cre* mice into irradiated Ly5.1$^+$ hosts. Prior to transfer, the BM was depleted of Ter119$^+$, IgM$^+$, and CD5$^+$ cells. For a control, we also transferred BM cells from adult Ly5.2$^+$ *Ptpn6*$^{+/+}$;CD19-*cre* mice after similar depletion into another cohort of irradiated Ly5.1$^+$ hosts. Less than 2% of the cells were Ig$^+$ in the immuno-depleted BM (Figures 4A and 4B). The resulting chimeras had donor (Ly5.2$^+$) IgM$^+$ B and CD5$^+$ T cells (Figure 4C) in their spleens (upper panels), lymph nodes (middle panels), and peritoneum (lower panels). Although fewer *Ptpn6*$^{f/f}$;CD19-*cre*-derived IgM$^+$ cells than *Ptpn6*$^{+/+}$;CD19-*cre*-derived IgM$^+$ cells were found in the spleen, the opposite was observed in the peritoneum (Figure 4D). Furthermore, the percentages of donor-derived IgM$^+$CD5$^+$ cells in the spleen and peritoneum of *Ptpn6*$^{f/f}$;CD19-*cre* chimeras were greater than those found in *Ptpn6*$^{+/+}$;CD19-*cre* chimeras (Figure 4E). We also sequenced the $V_{HJ558}D$ and DJ_{H1} junctions in splenic CD5$^+$ and CD5$^-$ B cells isolated from 6-month-old *Ptpn6*$^{f/f}$;CD19-*cre* mice and found that these B cells contained N nucleotide additions (Table S1). Taken together, these findings strongly suggest an adult origin for the B-1a cells in *Ptpn6*$^{f/f}$;CD19-*cre* mice.

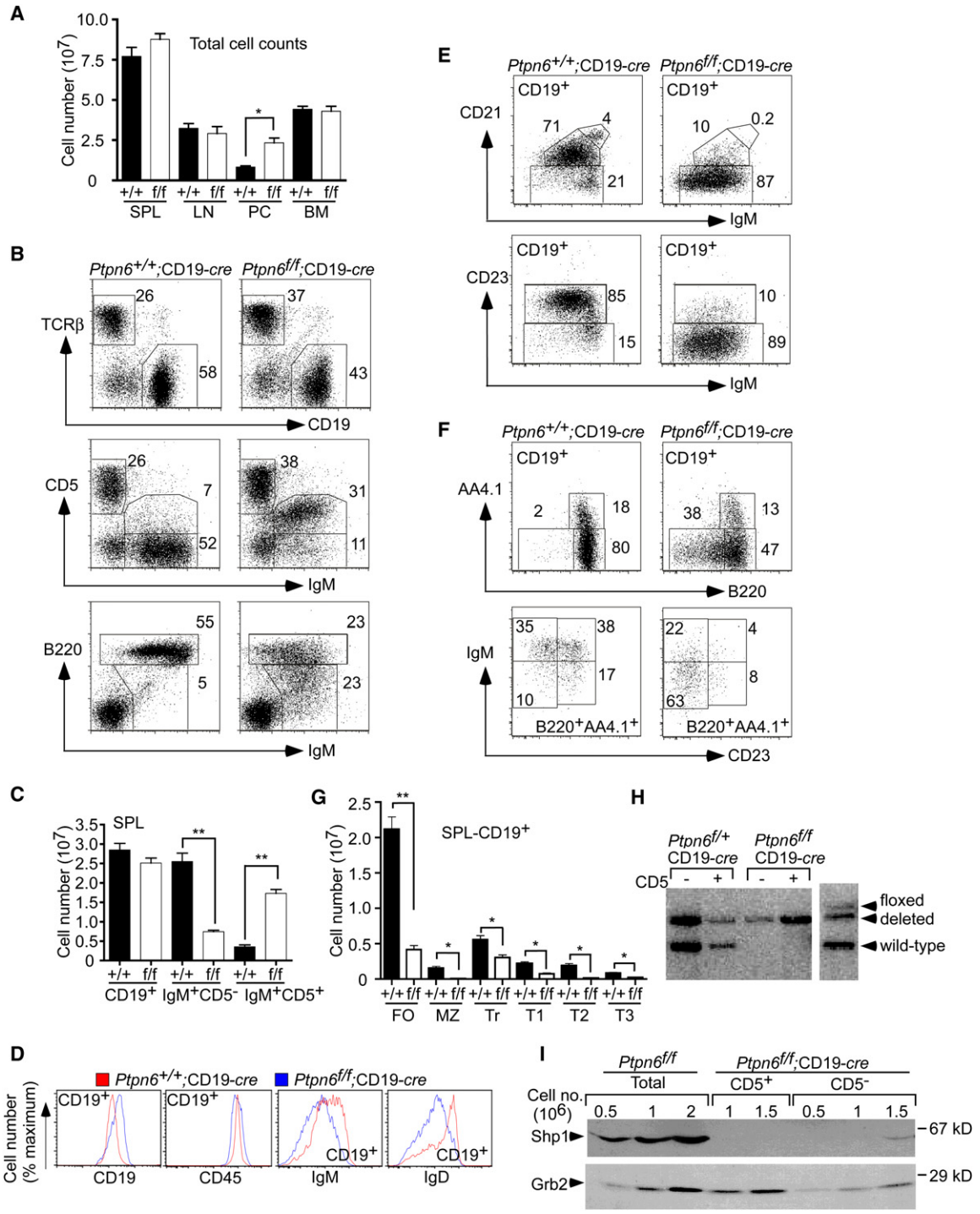

Figure 2. Effects of B Cell-Specific *Ptpn6* Deletion on Splenic B Cells

(A) Total spleen (SPL), peripheral lymph node (LN), peritoneal exudate (PC), and BM cells recovered from 11- to 12-week-old *Ptpn6*$^{+/+}$;CD19-*cre* (filled bars) and *Ptpn6*$^{f/f}$;CD19-*cre* (open bars) mice (n = 4 each), plotted as mean ± SEM. *p < 0.05, paired two-tailed t test.

(B) *Ptpn6*$^{+/+}$;CD19-*cre* (left) and *Ptpn6*$^{f/f}$;CD19-*cre* (right) splenocytes, stained for expression of the indicated markers. Numbers represent percentages of cells within the lymphocyte gate, representative of at least six experiments.

(C) Absolute numbers of CD19$^+$, IgM$^+$CD5$^-$, and IgM$^+$CD5$^+$ splenocytes from *Ptpn6*$^{+/+}$;CD19-*cre* (filled bars) and *Ptpn6*$^{f/f}$;CD19-*cre* (open bars) mice (n = 4 each), plotted as mean ± SEM. **p < 0.005 by paired two-tailed t test.

(D) Histograms of CD19, CD45, IgM, and IgD levels on CD19$^+$ splenic B cells from *Ptpn6*$^{+/+}$;CD19-*cre* (red) and *Ptpn6*$^{f/f}$;CD19-*cre* (blue) mice. Data represent at least five experiments.

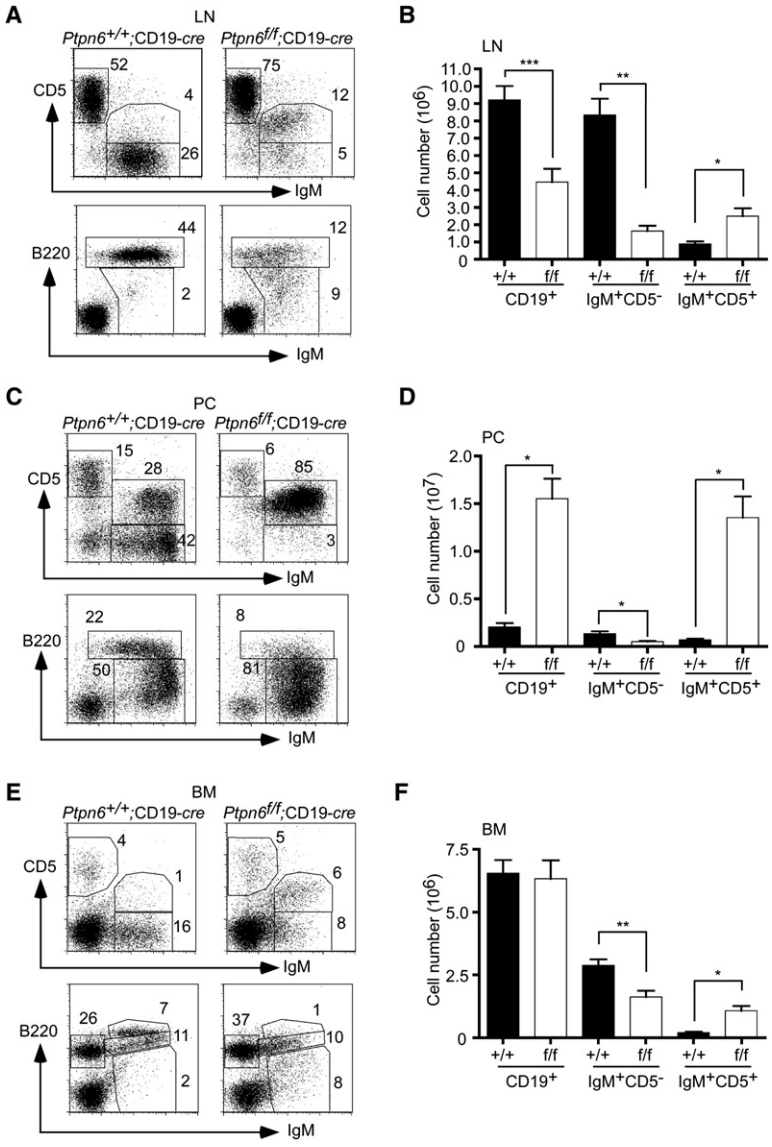

Figure 3. Effects of B Cell-Specific *Ptpn6* Deletion on Other Lymphoid Populations

(A) Flow cytometry of lymph node (LN) cells from 11- to 12-week-old *Ptpn6*$^{+/+}$;CD19-*cre* (left) and *Ptpn6*$^{f/f}$;CD19-*cre* (right) mice, stained for surface IgM, CD5, and B220. Numbers represent percentages of cells within the lymphocyte gate, representing at least four experiments.

(B) Absolute numbers of LN CD19$^+$, IgM$^+$CD5$^-$ and IgM$^+$CD5$^+$ B cells from *Ptpn6*$^{+/+}$;CD19-*cre* (filled bars) and *Ptpn6*$^{f/f}$;CD19-*cre* (open bars) mice (n = 4 each), plotted as mean ± SEM. *p < 0.05; **p < 0.005; ***p < 0.0005 by paired two-tailed t test.

(C) Peritoneal (PC) cells from 11- to 12-week-old *Ptpn6*$^{+/+}$;CD19-*cre* (left) and *Ptpn6*$^{f/f}$;CD19-*cre* (right) mice, stained for surface IgM, CD5, and B220. Numbers represent percentages of cells within the lymphocyte gate; representative of at least ten experiments.

(D) Absolute numbers of PC CD19$^+$, IgM$^+$CD5$^-$, and IgM$^+$CD5$^+$ B cells from *Ptpn6*$^{+/+}$;CD19-*cre* (filled bars) and *Ptpn6*$^{f/f}$;CD19-*cre* (open bars) mice (n = 4 each), plotted as mean ± SEM. *p < 0.05 by paired two-tailed t test.

(E) BM cells from 11- to 12-week-old *Ptpn6*$^{+/+}$;CD19-*cre* (left) and *Ptpn6*$^{f/f}$;CD19-*cre* (right) mice stained for surface IgM, CD5, and B220, representing at least six experiments.

(F) Absolute numbers of BM CD19$^+$, IgM$^+$CD5$^-$ and IgM$^+$CD5$^+$ B cells from *Ptpn6*$^{+/+}$;CD19-*cre* (filled bars) and *Ptpn6*$^{f/f}$;CD19-*cre* (open bars) mice (n = 4 each), plotted as mean ± SEM. *p < 0.05; **p < 0.005 by paired two-tailed t test.

Altered Antibody Responses in *Ptpn6*$^{f/f}$;CD19-*cre* Mice

Similar to *motheaten* mice (Shultz, 1998), younger (8- to 15-week-old) *Ptpn6*$^{f/f}$;CD19-*cre* mice had increased serum IgM, IgG_{2a}, and IgG_3, whereas IgA, IgG_1, and IgG_{2b} concentrations were not altered significantly (Figure 5A). However, unlike *motheaten* mice (Sidman et al., 1986), *Ptpn6*$^{f/f}$;CD19-*cre* mice did not show augmented usage of λ light chains in serum antibodies or surface Ig (data not shown).

To determine the ability of *Ptpn6*$^{f/f}$;CD19-*cre* mice to mount specific antibody responses, groups of 8-week-old mice were immunized with either a thymus-dependent (TD; NP_{18}-CG) or a thymus-independent type II (TI-II;

(E) Representative analysis of splenocytes stained with CD19, IgM, CD21, and CD23 antibodies. Numbers indicate percentages of cells within the CD19$^+$ gate.

(F) Representative analysis of splenocytes stained with CD19, IgM, AA4.1, B220, and CD23 antibodies. Numbers indicate percentages of cells within the CD19$^+$ gate (upper) or CD19$^+$B220$^+$AA4.1$^+$ gate (lower).

(G) Quantification of splenic B cell subsets as shown in (E) and (F) from *Ptpn6*$^{+/+}$;CD19-*cre* (filled bars) and *Ptpn6*$^{f/f}$;CD19-*cre* (open bars) mice (n = 4 each), plotted as mean ± SEM. *p < 0.05; **p < 0.005, paired two-tailed t test.

(H) Southern blot, showing deletion efficiency in IgM$^+$CD5$^-$ and IgM$^+$CD5$^+$ splenic B cells from the indicated mice. DNA from *Ptpn6*$^{f/+}$;*Mx1-cre* splenocytes with incomplete deletion of the Shp1 locus was resolved on the same gel (right-most lane), to indicate floxed, deleted, and wild-type alleles, respectively.

(I) Shp1-protein amounts in *Ptpn6*$^{f/f}$;CD19-*cre* splenic B cells. The indicated numbers of IgM$^+$CD5$^+$ and IgM$^+$CD5$^-$ cells were lysed, immunoblotted for Shp1, and reprobed for Grb2 to control for loading.

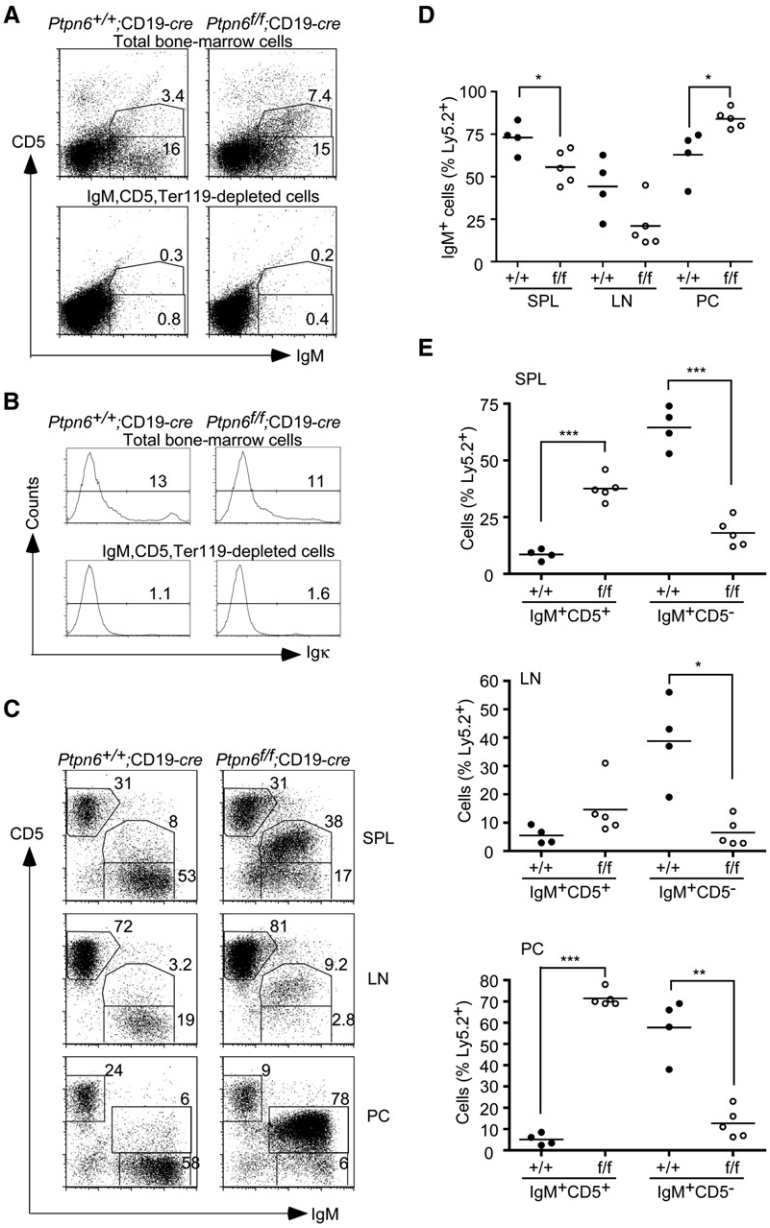

Figure 4. Adult Origin of B-1a Cells in Mice with B Cell-Specific *Ptpn6* Deletion

(A) BM predepletion (upper panels) and post-depletion (lower panels) of IgM$^+$, CD5$^+$, and Ter119$^+$ cells from 11- to 12-week-old Ly5.2$^+$ *Ptpn6*$^{+/+}$;CD19-*cre* (left) and *Ptpn6*$^{f/f}$;CD19-*cre* (right) mice, stained for IgM and CD5. Numbers represent percentages of cells within the total live cell gate; data are representative of three experiments.

(B) Flow cytometry of BM prepared as shown in (A), stained for Igκ.

(C) Splenocytes (SPL), LN cells, and peritoneal exudates (PC) from Ly5.1$^+$ mice 8 weeks after reconstitution with IgM$^+$-, CD5$^+$-, and Ter119$^+$-depleted BM from 11- to 12-week-old Ly5.2$^+$ *Ptpn6*$^{+/+}$;CD19-*cre* (left) and *Ptpn6*$^{f/f}$;CD19-*cre* (right) mice, stained for IgM and CD5. Numbers indicate percentages of cells within the Ly5.2$^+$ lymphocyte gate. In the *Ptpn6*$^{+/+}$;CD19-*cre* chimera shown, Ly5.2$^+$ cells were 50%, 54%, and 50% of total lymphocytes recovered from spleen, LN, and peritoneum, respectively. For the *Ptpn6*$^{f/f}$;CD19-*cre* chimera, Ly5.2$^+$ cells were 84%, 83%, and 93% of total lymphocytes recovered from the same sites, respectively.

(D) Quantification of Ly5.2$^+$ donor-derived IgM$^+$ cells in (C) from *Ptpn6*$^{+/+}$;CD19-*cre* (filled circles, n = 4) and *Ptpn6*$^{f/f}$;CD19-*cre* (open circles, n = 5) mice. Each symbol represents an individual chimera, with the bar indicating the mean percentage. *p < 0.05 by unpaired two-tailed t test.

(E) Quantification of Ly5.2$^+$ donor-derived IgM$^+$CD5$^+$ and IgM$^+$CD5$^-$ cells in (C) from *Ptpn6*$^{+/+}$;CD19-*cre* (filled circles, n = 4) and *Ptpn6*$^{f/f}$;CD19-*cre* (open circles, n = 5) mice. Each symbol represents an individual chimera. The bar indicates the mean percentage. *p < 0.005; **p < 0.0005; ***p < 0.0001 by unpaired two-tailed t test.

NP_{25}-Ficoll) antigen. Even prior to immunization (day 0), sera from *Ptpn6*$^{f/f}$;CD19-*cre* mice contained elevated amounts of κ bearing Ig and IgM that cross-reacted with NP-BSA (Figures 5B and 5C). Mutant mice responded to NP-CG, as shown by an increase of NP-binding IgM and IgG_1 as well as total κ or λ light-chain-bearing antibodies in their sera on days 7, 14, and 21 after immunization, but the magnitude of the increase was lower than that in control mice (Figure 5B). The response of *Ptpn6*$^{f/f}$;CD19-*cre* mice to NP-Ficoll immunization was severely impaired (Figure 5C). No NP-specific IgM or IgG_1 response could be detected in immunized mutant mice, and the IgG_3 response was drastically reduced compared to controls (Figure 5C), indicating a compromised ability of Shp1-deficient B cells to react against TD and TI-II antigens.

B Cell-Specific-Shp1 Deficiency Affects Proliferation and Calcium Mobilization

To investigate why *Ptpn6*$^{f/f}$;CD19-*cre* mice cannot mount an effective antigen response, we assessed the ability of purified CD19$^+$ B cells (which include B-1 and B-2 cells) from control *Ptpn6*$^{f/+}$;CD19-*cre* and *Ptpn6*$^{f/f}$;CD19-*cre* spleens to respond to various stimuli. Compared to controls, *Ptpn6*$^{f/f}$;CD19-*cre* B cells proliferated substantially less upon stimulation by anti-IgM or anti-CD40, as well as by combinations of anti-IgM with anti-CD40 or IL-4. LPS-evoked proliferation was similar in control and Shp1-deficient splenic B cells, indicating that Shp1-deficient B cells are not intrinsically unable to proliferate in culture and that Toll-like receptor 4 signaling is normal (Figure 6A).

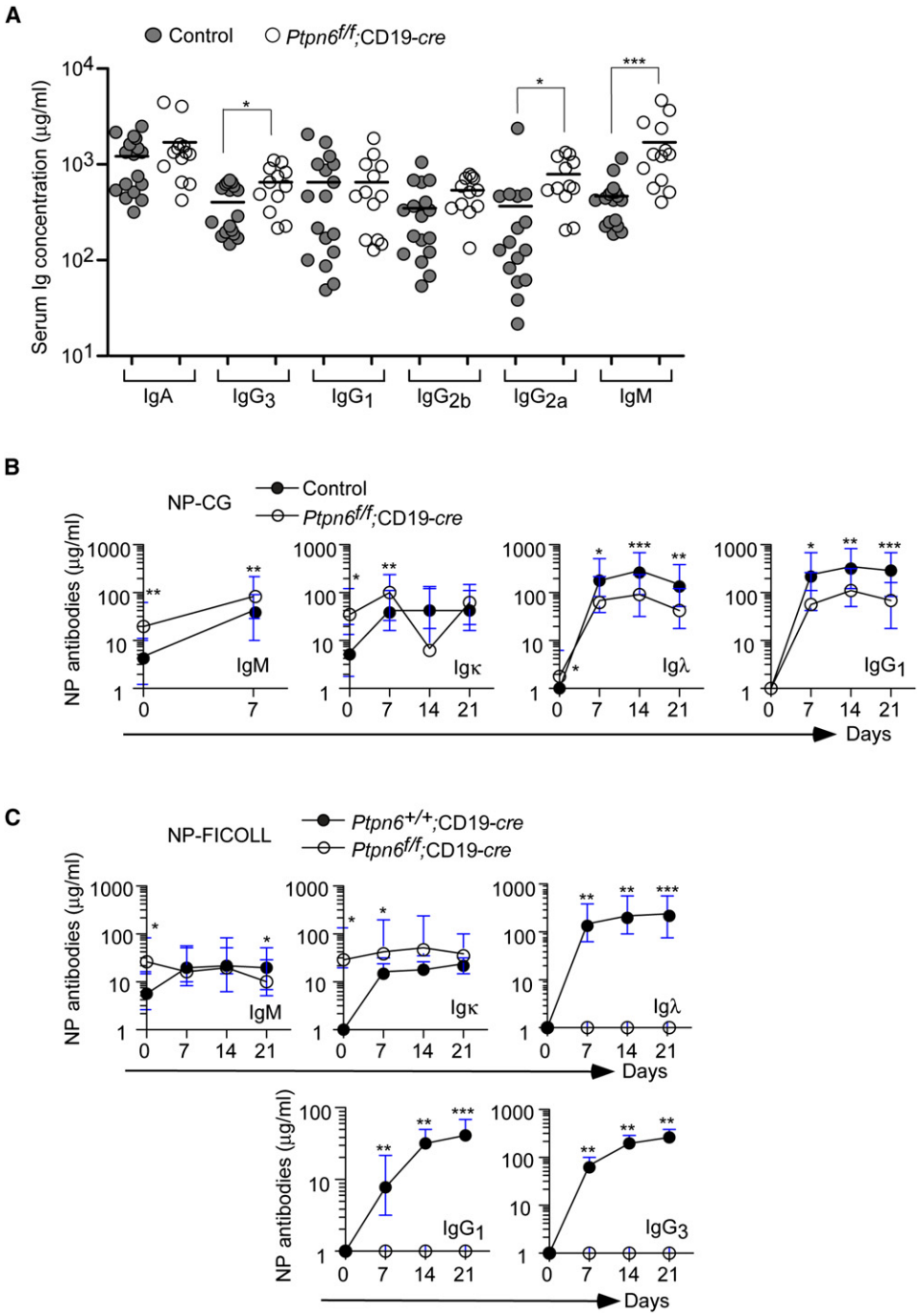

Figure 5. Altered B Cell Function in Serum Ig Production and Humoral Responses

(A) Antibody titers from 8-week-old control (filled circles, n = 16) and *Ptpn6*$^{f/f}$;CD19-*cre* (open circles, n = 12) mice. Controls include *Ptpn6*$^{f/f}$, *Ptpn6*$^{f/+}$, *Ptpn6*$^{f/+}$;CD19-*cre*, and *Ptpn6*$^{+/+}$;CD19-*cre* mice. Each symbol represents an individual mouse. The bar indicates the mean titer. *p < 0.05; ***p < 0.0005 by Wilcoxon one-tailed t test.

(B) T cell-dependent immune response. Groups of eight control and six *Ptpn6*$^{f/f}$;CD19-*cre* mice were immunized with 50 μg NP_{18}-CG in alum and bled before (day 0) and on days 7, 14, and 21 postimmunization. NP-specific titers were determined by ELISA and plotted as the geometric mean ± 95% confidence intervals (CI). Filled circles represent control mice; open circles represent *Ptpn6*$^{f/f}$;CD19-*cre* mice. Points on the x axis are below the detection limit. *p < 0.05; **p < 0.005; ***p < 0.0005 by unpaired one-tailed t test.

(C) T cell-independent immune response. *Ptpn6*$^{+/+}$;CD19-*cre* and *Ptpn6*$^{f/f}$;CD19-*cre* mice (n = 4 each) were immunized with 20 μg of NP_{25}-Ficoll in PBS, and NP-specific titers on days 0, 7, 14, and 21 were determined by ELISA. Data are plotted as the geometric mean ± 95% CI. Filled circles represent *Ptpn6*$^{+/+}$;CD19-*cre* mice; open circles represent *Ptpn6*$^{f/f}$;CD19-*cre* mice. For IgG_1, points on the x axis are below the detection limit. *p < 0.05; **p < 0.005; ***p < 0.0005 by unpaired one-tailed t test.

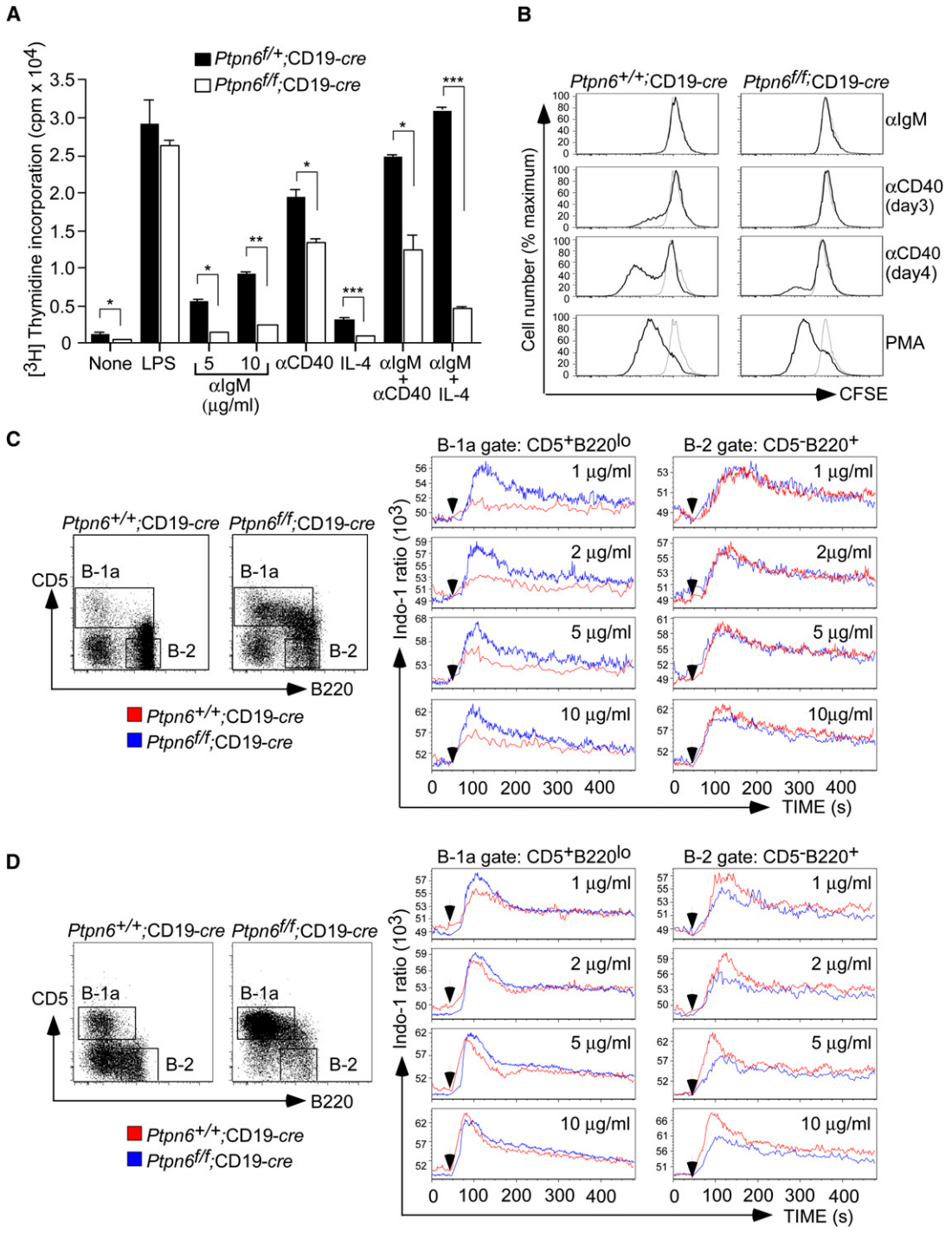

Figure 6. B Cell Responses in *Ptpn6*$^{f/f}$;CD19-*cre* Mice

(A) Ex vivo proliferation of splenic B cells. CD19$^+$ B cells from 9- to 10-week-old *Ptpn6*$^{f/+}$;CD19-*cre* and *Ptpn6*$^{f/f}$;CD19-*cre* mice were cultured with LPS (10 μg/ml), IgM antibody (5 or 10 μg/ml, F(ab')$_2$), CD40 antibody (0.75 μg/ml), IL-4 (25 U/ml), or IgM antibody (5 μg/ml, F(ab')$_2$) together with either CD40 antibody (0.75 μg/ml) or IL-4 (25 U/ml), and [^{3}H] thymidine incorporation was assessed. One of two experiments with similar results is shown. Data are expressed as mean ± SEM. *p < 0.05; **p < 0.005; ***p < 0.0005 by paired two-tailed t test.

(B) Ex vivo proliferation of peritoneal B-1a cells. Histograms show CFSE intensities of peritoneal CD5$^+$CD19$^+$ B cells from 10- to 11-week-old *Ptpn6*$^{+/+}$;CD19-*cre* mice (left) and *Ptpn6*$^{f/f}$;CD19-*cre* mice (right) 3 days after culture, unless otherwise indicated. Cells were either left unstimulated (gray line) or were stimulated (black line) with 10 μg/ml IgM antibody (F(ab')$_2$, top), 2.5 μg/ml CD40 antibody (middle two), or 0.3 μg/ml PMA (bottom). One of two experiments with similar results is shown.

(C) Calcium response in splenic B cells. Splenocytes were stimulated with IgM antibody (F(ab')$_2$, 1, 2, 5, or 10 μg/ml) at the indicated time (arrow) for 8 min. Intracellular calcium concentrations of splenic CD5$^+$B220^{lo} B-1a cells (middle panels) and splenic CD5$^-$B220$^+$ B-2 cells (right panels) from 11- to

Normal B-1a cells fail to proliferate in response to anti-IgM and, in contrast to B-2 cells, proliferate upon treatment with phorbol esters (Berland and Wortis, 2002). Hence, the apparent impairment of the anti-IgM-evoked proliferative response in splenic B cells from *Ptpn6*$^{f/f}$;CD19-*cre* mice could reflect their predominantly B-1a phenotype, rather than an intrinsic difference in BCR signaling in Shp1-deficient cells. Indeed, like normal B-1a cells, Shp1-deficient peritoneal B-1a cells proliferated in response to PMA and failed to respond to anti-IgM stimulation (Figure 6B). However, unlike normal B-1a cells, which responded to anti-CD40 stimulation, the anti-CD40-evoked response of Shp1-deficient peritoneal B-1a cells was greatly reduced (Figure 6B).

We also assessed the ability of splenic B cells in *Ptpn6*$^{f/f}$;CD19-*cre* mice to mobilize calcium upon IgM cross-linking. Because of the intrinsic signaling differences between B-1 and B-2 cells (Berland and Wortis, 2002), we examined CD5$^+$ and CD5$^-$ B cells separately. Upon anti-IgM stimulation, splenic CD5$^+$B220^{lo} B-1a cells from *Ptpn6*$^{f/f}$;CD19-*cre* mice exhibited a greater increase in intracellular calcium concentration than their counterparts from *Ptpn6*$^{+/+}$;CD19-*cre* mice (Figure 6C). In contrast, splenic CD5$^-$B220$^+$ B-2 cells from *Ptpn6*$^{+/+}$;CD19-*cre* and *Ptpn6*$^{f/f}$;CD19-*cre* mice exhibited comparable IgM-mediated calcium responses (Figure 6C); the incomplete ablation of Shp1 protein in these cells (Figure 2I) could contribute to this finding. Similar to splenic B-1a cells, peritoneal CD5$^+$B220^{lo} B-1a cells from *Ptpn6*$^{f/f}$;CD19-*cre* mice also exhibited an increased response as compared to peritoneal B-1a cells from *Ptpn6*$^{+/+}$;CD19-*cre* mice, but this enhancement was very modest and detectable only at lower doses of stimulation (Figure 6D). Unexpectedly, peritoneal CD5$^-$B220$^+$ B-2 cells from *Ptpn6*$^{f/f}$;CD19-*cre* mice exhibited a decreased response compared to such cells from *Ptpn6*$^{+/+}$;CD19-*cre* mice, suggesting that Shp1 may positively regulate BCR signaling in B-2 cells under certain circumstances (Figure 6D).

Old *Ptpn6*$^{f/f}$;CD19-*cre* Mice Develop Autoimmunity

Compared to age-matched controls, older (5–6 month) *Ptpn6*$^{f/f}$;CD19-*cre* mice had increased serum titers of IgM, IgG$_{2a}$, and IgG$_1$ antibodies reactive to single stranded (ss) DNA (Figure 7A). *Ptpn6*$^{f/f}$;CD19-*cre* mice also had elevated titers of IgM and IgG$_{2a}$ against double stranded (ds) DNA (Figure 7B). Both κ and λ light chains were associated with these autoantibodies against DNA (Figures 7A and 7B).

Autopsies of 7- to 11-month-old *Ptpn6*$^{f/f}$;CD19-*cre* mice revealed multiple abnormalities, including enlarged spleens and lymph nodes (Figure S5). Flow-cytometric analysis of cells from these organs revealed increased numbers of B and T lymphocytes, macrophages, and granulocytes (data not shown). This is distinct from the *motheaten* mice's hypercellularity, which mainly reflects extramedullary hematopoiesis (Shultz, 1998). Hematoxylin and eosin (H and E) staining of spleen and lymph-node sections revealed increased numbers of plasma and Mott cells (data not shown). Predominantly lymphocytic infiltrates also were seen in liver and lungs (Figures 7C$_b$ and 7C$_d$) and, accordingly, immunostaining revealed large numbers of B220$^+$ B cells and CD3$^+$ T cells in the lung (Figures 7D$_b$ and 7D$_d$) and B220$^+$ infiltrates in the liver (Figure 7D$_f$). These findings differ from the motheaten phenotype, which features myeloid infiltrates in these tissues (Shultz, 1998). Increased B220$^+$ cells also were found in the thymic cortex (Figure 7D$_h$), in contrast to the early thymic atrophy seen in *motheaten* mice (Shultz, 1998). Renal sections revealed glomerulonephritis (Figure 7C$_f$), and electron microscopy showed mesangial deposits of fine, granular, electron-dense material (Figure 7E, asterisks), which stained positive for IgM (Figure 7E, lower panel), consistent with immune-complex deposition. Thus, deletion of *Ptpn6* only in B cells eventually leads to the development of an autoimmune disease with features similar to systemic lupus erythematosus (SLE).

DISCUSSION

The complexity of the motheaten phenotype has hindered efforts to define the primary effects of Shp1 deficiency in B cells. By analyzing mice with B cell-specific *Ptpn6* deletion, we have identified B cell-autonomous and nonautonomous effects of Shp1. The dramatic increase in B-1a cells at the expense of B-2 cells in *Ptpn6*$^{f/f}$;CD19-*cre* mice indicates that Shp1 deficiency affects this phenotype in a cell-autonomous fashion. Unlike *motheaten* mice, however, *Ptpn6*$^{f/f}$;CD19-*cre* mice do not have increased serum IgG$_1$, IgG$_{2b}$, and IgA titers (Sidman et al., 1986). Although the mechanism for the increase in serum IgG$_{2a}$ in *motheaten* and *Ptpn6*$^{f/f}$;CD19-*cre* mice is unclear, elevated IgM and IgG$_3$ could be due to the increase in B-1a cells, which normally produce these isotypes (Berland and Wortis, 2002). Because isotype switching requires T cells, Shp1 deficiency in T and antigen-presenting cells may contribute to the enhanced serum IgG and IgA titers in *motheaten* mice. The reported hyperproliferative response of *motheaten* splenic B cells to anti-Ig stimulation (Pani et al., 1995) also is not B cell autonomous. Instead, B cell-specific Shp1 deficiency actually reduces anti-IgM-induced splenic B cell proliferation, probably reflecting the great percentage of B-1a cells in *Ptpn6*$^{f/f}$;CD19-*cre* mice and the intrinsically different responses of B-1a and B-2 cells to anti-IgM stimulation (Berland and Wortis, 2002). Previous studies of *motheaten* B cells did not assess CD40-mediated proliferation. Unexpectedly, we find that such responses are diminished in peritoneal *Ptpn6*$^{f/f}$;CD19-*cre* B-1a cells, by a mechanism

12-week-old *Ptpn6*$^{+/+}$;CD19-*cre* (red) and *Ptpn6*$^{f/f}$;CD19-*cre* (blue) mice are presented as the ratio of bound to unbound Indo-1. B-1a and B-2 gates were drawn as indicated in the dot plots (left).

(D) Calcium response in peritoneal B cells. PC cells were stimulated with IgM antibodies and their calcium responses assessed as in (C). Anti-B220 and anti-CD5 pretreatment had no effect on calcium flux (data not shown). Data shown are representative of three independent experiments.

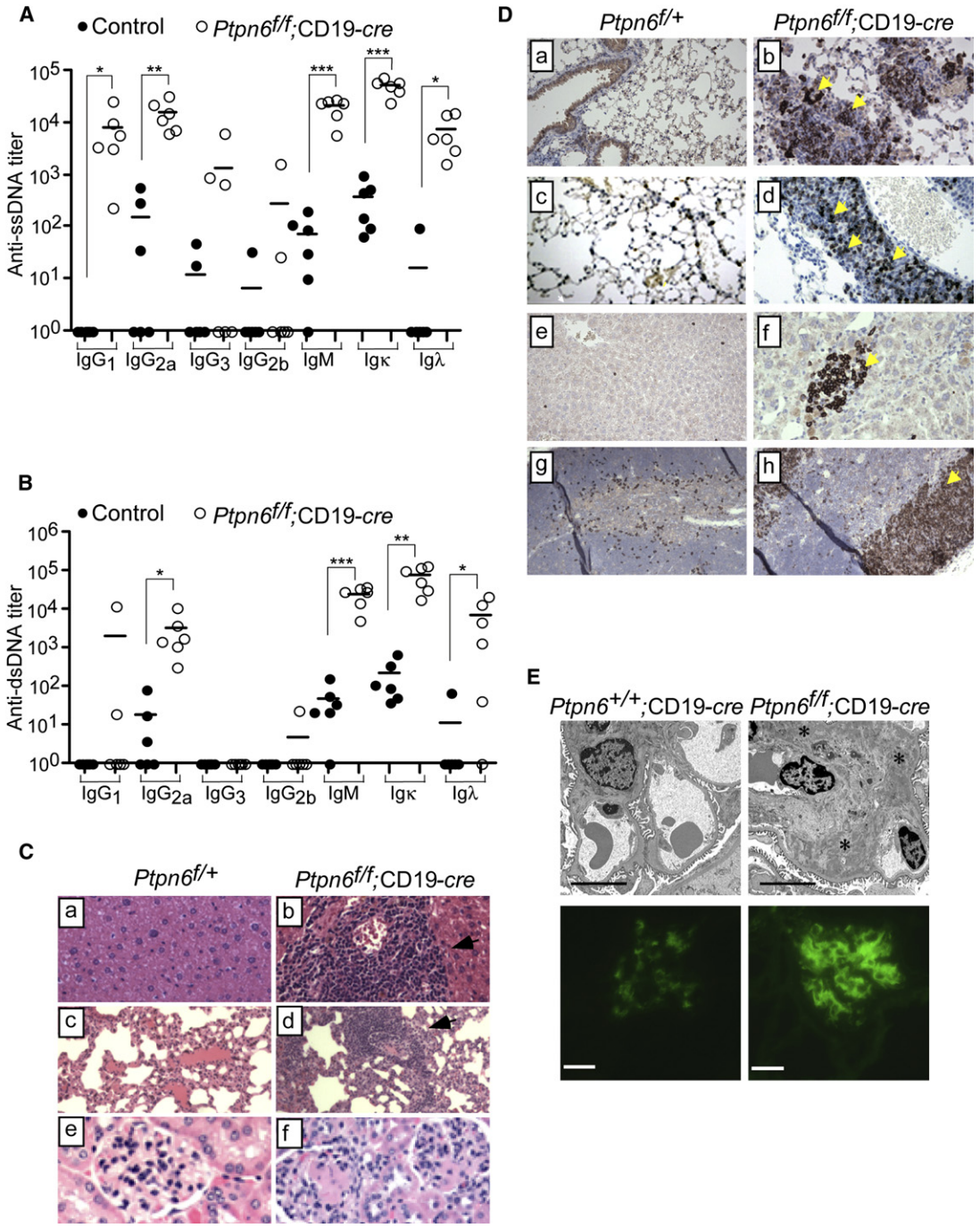

Figure 7. Autoimmunity in *Ptpn6*$^{f/f}$;CD19-*cre* Mice

(A) ssDNA antibody titers in sera of 5- to 7-month-old control (filled circles, n = 6) and *Ptpn6*$^{f/f}$;CD19-*cre* (open circles, n = 6) mice. Each symbol represents one animal. Titers below the detection limit are plotted on the x axis. *$p < 0.05$; **$p < 0.005$; ***$p < 0.0001$, unpaired one-tailed t test.

(B) dsDNA antibodies in the sera of 5- to 7-month-old control (filled circles, n = 6) and *Ptpn6*$^{f/f}$;CD19-*cre* (open circles, n = 6) mice. *$p < 0.05$; **$p < 0.005$; ***$p < 0.0005$, unpaired one-tailed t test.

(C) H and E stained sections of liver (C_a and C_b), lungs (C_c and C_d), and kidney (C_e and C_f) from 8-month-old *Ptpn6*$^{f/+}$ (C_a, C_c, and C_e) and *Ptpn6*$^{f/f}$;CD19-*cre* (C_b, C_d, and C_f) mice. Black arrows indicate cellular infiltrates. Liver and kidney sections are shown at 200×; lung sections are at 100×. Data represent six mice (7 to 11 month old) of each genotype.

(D) IHC (200×) of lungs (D_a–D_d), liver (D_e and D_f) and thymus (D_g and D_h) from 7-month-old *Ptpn6*$^{f/+}$ (D_a, D_c, D_e, and D_g) and *Ptpn6*$^{f/f}$;CD19-*cre* (D_b, D_d, D_f, and D_h) mice, stained with B220 (D_a, D_b, and D_e–D_h) or CD3 antibodies (D_c and D_d). Reactive cells are red/brown (yellow arrows). Data represent one of two mice of each genotype with similar results.

yet to be determined. *Ptpn6*$^{f/f}$;CD19-*cre* mice also showed impaired antibody responses to antigenic challenges. To our knowledge, no such studies with the *motheaten* mice have been reported. Although B-1 cells are involved in T1-II responses (reviewed in Berland and Wortis [2002]), they do not respond to NP-Ficoll, as used in this study (Förster and Rajewsky, 1987). Instead, MZ B cells appear to respond to this antigen (Guinamard et al., 2000), so the impaired NP-Ficoll response in *Ptpn6*$^{f/f}$;CD19-*cre* mice could reflect their reduced MZ population. How Shp1 deficiency in B cells affects the TD response is not clear. The responding population (B-2 cells) is reduced in *Ptpn6*$^{f/f}$;CD19-*cre* mice and shows incomplete *Ptpn6* deletion. Thus, the impaired TD response in *Ptpn6*$^{f/f}$;CD19-*cre* mice may reflect a reduced number of responding cells, rather than impaired responsiveness due to Shp1 deficiency. Whether Shp1-deficient B-1a cells in *Ptpn6*$^{f/f}$;CD19-*cre* mice also contribute to TD response remains unknown. Finally, *Ptpn6*$^{f/f}$;CD19-*cre* mice develop systemic autoimmunity, characterized by polyreactive autoantibodies, tissue infiltration with lymphoid cells, and immune-complex glomerulonephritis, suggesting that Shp1-deficiency in B cells alone is sufficient to elicit this pathology. Whereas the disease occurs in *Ptpn6*$^{f/f}$;CD19-*cre* mice only at >5 months of age, *motheaten* mice exhibit such abnormalities within 3 weeks of birth. Thus, absence of Shp1 in other cell types clearly contributes to the full autoimmune phenotype in *motheaten* mice.

Cell-transfer studies demonstrate the propensity of fetal precursors to generate B-1a cells (Herzenberg et al., 1986), although adult BM progenitors can generate B-1a cells at low frequency (Berland and Wortis, 2002). The identification of Lin$^-$B220$^-$CD19$^+$AA4.1$^+$ B-1 cell precursors in adult BM suggests that B-1a cells are not exclusively fetal liver derived (Montecino-Rodriguez et al., 2006). We found that recipients of adult *Ptpn6*$^{f/f}$;CD19-*cre* BM have abundant donor-derived B-1a cells. Thus, Shp1-deficient B-1a cells, like wild-type B-1a cells, can be generated from progenitors found in adult BM, a contention supported by the similar extent of N nucleotide addition in wild-type (Gu et al., 1990; Gu et al., 1992) and Shp1-deficient B-1a cells from mice of similar age.

Preliminary experiments indicate that adult *Ptpn6*$^{f/f}$;CD19-*cre* mice have a normal number of Lin$^-$B220$^-$CD19$^+$AA4.1$^+$ BM B-1 progenitors (data not shown), which suggest that Shp1 deficiency may lead to expansion of B-1a cells as they develop. However, the increased number of splenic B-1a cells in *Ptpn6*$^{f/f}$;CD19-*cre* mice occurs at the expense of B-2 cells. Splenic B-1a and residual B-2 cells found in *Ptpn6*$^{f/f}$;CD19-*cre* mice have different extents of Shp1 deletion, with low amounts of Shp1 protein still detectable in B-2 cells. Conceivably as Shp1-protein amounts decline in developing B-2 cells in *Ptpn6*$^{f/f}$;CD19-*cre* mice (i.e., after CD19-*cre*-mediated excision of the floxed *Ptpn6* allele), cells initially destined to become B2 cells may be redirected into the B-1a pathway. Alternatively, Shp1 deficiency could selectively promote survival or expansion of B-1a cells while causing the death of B-2 cells.

Numerous studies identify BCR signal strength as a critical determinant of B-1a cell development or maintenance. Although both *motheaten* and *Ptpn6*$^{f/f}$;CD19-*cre* mice have increased number of B-1a cells, BM from *motheaten* mice expressing an Ig transgene recognizing hen-egg lysozyme (HEL) gives rise to splenic B cells with a B-2 phenotype (Cyster and Goodnow, 1995). In the presence of soluble HEL, these motheaten-derived Ig^{HEL} B cells are deleted rather than anergized, suggesting that Shp1 deficiency does increase signaling strength.

Likewise, we find that Shp1 negatively regulates BCR-evoked calcium response in splenic and peritoneal CD5$^+$ B-1a cells, albeit to a different extent. Unexpectedly, whereas splenic CD5$^-$ B-2 cells from *Ptpn6*$^{f/f}$;CD19-*cre* mice responded normally to anti-IgM, their peritoneal counterparts had a reduced response. These findings are difficult to interpret, because the compositions of CD5$^-$ B cell compartment (e.g., B-1b, Tr, FO, and MZ) in *Ptpn6*$^{+/+}$;CD19-*cre* mice differ from those in *Ptpn6*$^{f/f}$;CD19-*cre* mice, and the analysis is further complicated by incomplete Shp1 depletion in this fraction. Shp1 deficiency in B-2 cells also may enhance BCR-mediated calcium flux. *Motheaten*-derived Ig^{HEL} splenic B cells, which are B-2 in phenotype, reportedly have enhanced BCR-evoked calcium flux compared to their wild-type counterparts (Cyster and Goodnow, 1995). However, the possibility that the elevated response in *motheaten*-derived Ig^{HEL} B cells reflects non-cell-autonomous effects of Shp1 deficiency cannot be excluded.

Although Shp1 may directly associate with the BCR (Pani et al., 1995), the signal-attenuating effects of Shp1 are believed to be mediated primarily via its binding to inhibitory receptors (Neel et al., 2003). B cells express several such receptors, including CD72, CD22, and paired Ig-like receptor (PIR)-B (Pritchard and Smith, 2003); in addition, B-1a cells express the inhibitory receptor CD5 (Berland and Wortis, 2002). The phenotypes of mice lacking these inhibitory receptors reveal both similarities to and differences from the effects of B cell-specific Shp1 deficiency in B-1a cell development, IgM-induced calcium flux, and proliferative responses (Bikah et al., 1996; Lajaunias et al., 2002; Nitschke et al., 1997; O'Keefe et al., 1996; Otipoby et al., 1996; Pan et al., 1999; Sato et al., 1996a; Ujike et al., 2002). Indeed, Shp1 is likely to regulate different aspects of B cell biology via combinations of several different inhibitory receptors.

Ptpn6 deletion only in B cells causes autoantibody production and systemic autoimmunity. Autoimmunity was also reported in one line of mice lacking CD22 (O'Keefe et al., 1999), mice with FcγRII deficiency in B

(E) Electron micrographs (upper panels) of glomerular segments from 8-month-old *Ptpn6*$^{+/+}$;CD19-*cre* (left) and *Ptpn6*$^{f/f}$;CD19-*cre* (right) mice. Mesangial thickenings and deposits are indicated with asterisks. Scale bars represent 5 μm. Lower panels show immunofluorescence of glomerular segments from *Ptpn6*$^{+/+}$;CD19-*cre* (left panel) and *Ptpn6*$^{f/f}$;CD19-*cre* (right panel) mice, demonstrating the presence of IgM in mesangial deposits.

cells (Bolland and Ravetch, 2000), and mice overexpressing CD19 (Sato et al., 1996b). These findings, and our own, suggest that defects solely in B lymphoid lineage cells can break tolerance.

For Shp1, this conclusion hinges on the B lymphoid specificity of the CD19-*cre* transgene. Studies of CD19-*cre* mice involving a floxed eYFP reporter support the B cell specificity of CD19-*cre* and argue against CD19-*cre*-mediated excision in macrophages or other myeloid cells (Ye et al., 2003). However, others report CD19 expression in non-B cells, including c-Kit$^+$ peritoneal mast cells (Gommerman et al., 2000) and a minor population of CD11c$^+$ splenic dendritic cells (DCs) (Munn et al., 2004). We failed to detect any evidence (by PCR) of Shp1 deletion in BM-derived mast cells from *Ptpn6*$^{f/f}$;CD19-*cre* mice (data not shown). Furthermore, although we did detect a CD19$^+$CD11c^{hi} splenocyte population, these cells were IgM$^+$, thereby strongly suggesting a B cell origin (data not shown). Although we cannot formally exclude the possibility that bona fide CD19$^+$ mast cells or DCs exist, we believe that the reported CD19$^+$ "mast cells" and "DCs" represent rare B cells that express c-Kit and CD11c, respectively, and such cells could contribute to autoimmunity in older *Ptpn6*$^{f/f}$;CD19-*cre* mice. We also cannot exclude the possibility that the hybrid 129 × C57BL/6 background of *Ptpn6*$^{f/f}$;CD19-*cre* mice influences the pathogenesis and progression of the disease (Bygrave et al., 2004). Nevertheless, because we failed to observe autoimmunity in age-matched control mice on a similar mixed background, disease development clearly requires Shp1 deficiency in B cells.

How B cell-specific Shp1 deficiency lead to autoimmunity is unclear. Patients with SLE, also characterized by autoantibodies and immune-complex glomerulonephritis, have autoreactive and polyreactive BCRs in their mature, naive B cell repertoire. Normally, such BCRs are found in BM B cells and recent emigrants. These data implicate defective peripheral B cell tolerance in pathogenic antibody production in SLE (Yurasov et al., 2005). Conceivably, Shp1 deficiency affects peripheral tolerance, allowing the persistence of autoreactive and polyreactive B cells. Also, the B-1a cell repertoire may be altered significantly in Shp1-deficient mice. Although Shp1-deficient B cells are poorly responsive to anti-IgM or -CD40 stimulation ex vivo, they may respond to as yet unidentified ligands in vivo, leading to a breakdown of tolerance.

Our studies of the consequences of *Ptpn6* deletion have revealed the complexity of B cell-specific effects of Shp1 in controlling B-1a cell development and autoimmunity. Deletion of Shp1 in additional lymphohematopoietic cell compartments will provide a rational approach to decipher the complex cellular and molecular mechanisms underlying the inflammation and autoimmunity in *motheaten* mice.

EXPERIMENTAL PROCEDURES

Gene Targeting and Mice

A targeting vector (Figure S1), containing a *neo*^{r} cassette flanked by *loxP* sites in the 5′ untranslated region of *Ptpn6* exon I (II) and a *loxP* site in intron 9, was constructed by standard techniques. NotI-linearized targeting vector was electroporated into the 129Ola-derived ES cell line E14.1, and G418 and gancyclovir-resistant colonies were screened by Southern blotting with a flanking probe (Figure S1). Homologous recombinants were transiently transfected with a *cre*-encoding plasmid, and two *Ptpn6*$^{f/+}$ clones that had excised only the *neo*^{r} cassette were injected into blastocysts. The resulting chimeras were bred to C57BL/6 mice, and germline transmission was confirmed by Southern blotting. *Ptpn6*$^{f/+}$ mice were intercrossed to generate *Ptpn6*$^{f/f}$ or crossed to strains harboring CD19-*cre* (Rickert et al., 1997).

Mice and PCR Screening of *Ptpn6* Floxed and *cre* Alleles

All experiments used mice on mixed C57BL/6 × 129Ola background and, except where indicated, at 8–12 weeks of age. Floxed (~550 bp), deleted (~330 bp), and wild-type (~350 bp) *Ptpn6* alleles were identified by PCR with primers SHCP27 (5′ ACC-CTC-CAg-CTC-CTC-TTC), SHCP29 (5′ TgA-ggT-CCC-ggT-gAA-ACC), and SHCP32 (5′ TgT-TAT-gCA-TgT-gTg-TAT-Cg). Wild-type (452 bp) and *cre*-inserted (715 bp) *Cd19* alleles were identified by PCR with primers CD19c (5′ AAC-CAg-TCA-ACA-CCC-TTC-C), CD19d (5′ CCA-gAC-TAg-ATA-CAg-ACC-Ag) and Cre7 (5′ TCA-gCT-ACA-CCA-gAg-ACg-g). All mice used were maintained under specific pathogen-free conditions according to institutional guidelines and animal-study protocols approved by the institutional animal-care and -use committees.

Cell Preparation and Flow Cytometry

Single-cell suspensions of spleen and LN (cervical, auxillary, brachial, and inguinal) were prepared in RPMI + 2% FCS. The same medium was used to flush femurs and tibias and to lavage peritoneal cavities. Erythrocytes were lysed in 0.83% NH_4Cl/Tris-HCl (pH 7.2). Surface staining was performed on 1 × 10^6 cells in PBS, 2% FCS, and 0.2% azide on ice. Fluorochrome-conjugated or biotinylated B220 (RA3-6B2), IgM (II/4.1), IgD (1.3-5), TCRβ (H57−597), CD45 (30F11), Ly5.1 (A20), Ly5.2 (104), AA4.1, Gr-1 (RB6-8C5), CD19 (1D3), CD5 (53-7.3), CD23 (B3B4), CD21/35 (7G6), and CD43 (S7) monoclonal antibodies were used. IgM, TCRβ, Gr1, and AA4.1 antibodies were purchased from eBioscience; others were purchased from BD Biosciences. Flow-cytometric data were acquired on a FACScan, FACSCalibur, or LSRII (BD Biosciences) and analyzed with CellQuest Pro or FlowJo software.

Adoptive Transfer

Ly5.1$^+$ mice (7 to 9 week old) were irradiated with 950 rad and injected intravenously with 2 × 10^6 BM cells (predepleted for IgM$^+$, CD5$^+$, and Ter119$^+$ cells with biotinylated antibodies and biotin MACS) from 11- to 12-week-old *Ptpn6*$^{+/+}$;CD19-*cre* or *Ptpn6*$^{f/f}$;CD19-*cre* mice.

Ig Determinations

Serum IgM, IgA, IgG_1, IgG_2, and IgG_3 from tail-vein bleeds were quantified by ELISA, as described (Roes and Rajwesky, 1993). Sera were collected prior to intraperitoneal injection of antigen on day 0 and from immunized mice on days 7, 14, and 21. DNA antibodies were assayed in sera from 5- to 6-month-old mice, with plasmid DNA and boiled salmon-sperm DNA as sources of dsDNA and ssDNA, respectively.

Proliferation Assays

CD19 MACS (Miltenyi)-purified splenic B cells were cultured with stimuli at 2 to 3 × 10^5 cells per well in RPMI, 10% FCS, 2 mM glutamine, 1 mM sodium pyruvate, and 4.9 × 10^{-5} M 2-mercaptoethanol. After 36 hr, cells were pulsed with 1 μl Ci [methyl-^{3}H] thymidine for an additional 8 hr, and incorporation was quantified with a β-counter (Matrix 9600, Packard). B-1a cell proliferation was assessed by flow cytometry of CD5$^+$CD19$^+$ cells loaded with 5 μM carboxy-fluorescein diacetate and succinimidyl ester (CFSE, Molecular Probes) and cultured with stimuli for 3 or 4 days.

Calcium Flux

Cells were loaded with 5 μM Indo-1 AM (Molecular Probes) in RPMI and stained with B220-FITC, CD5-PE, CD4-APC, and CD8-APC antibodies. After exposure to F(ab)'$_2$ fragments of goat anti-mouse IgM (Jackson Immunoresearch) at 37°C, intracellular calcium concentrations in CD5$^-$B220$^+$ and CD5$^+$B220^{lo} cells were monitored for 8 min with an LSRII.

Histopathology

Tissues fixed with Bouin's solution or 10% formalin (Sigma) were stained with hematoxylin and eosin (H and E) or subjected to immunohistochemistry (IHC). B220 (BD Biosciences) and polyclonal CD3 (Dako) antibodies were used with methods previously described (Casola et al., 2004). Transmission electron microscopy was performed on kidney samples fixed in Karnovsky's media. Immunofluorescence was performed with FITC-conjugated goat antibodies against mouse IgA, IgG, and IgM and κ and λ light chains (Southern Biotech).

Statistical Analysis

All analyses were performed with Prism 4 program (GraphPad Software).

Supplemental Data

Five figures and one table are available at http://www.immunity.com/cgi/content/full/27/1/35/DC1/.

ACKNOWLEDGMENTS

We thank C. Göttlinger for cell sorting; C. Uthoff-Hachenberg for ELISA; A. Egert and A. Leinhaas for ES cell injection; K. Otipoby for insightful discussions; M. Schmidt-Supprian, D. Schenten and S. Koralov for reagents; and K. Swanson and M. Exley for critical reading of this manuscript. This work was supported by grants from the Human Frontier Science Program Organization, Deutsche Forschungsgemeinschaft through SFB 243, National Institutes of Health AI054636, the European Union through MUGEN (to K.R.), P01-DK50654, and R01-DK50693 (to B.G.N.). L.P. was supported by fellowships from the Alexander von Humboldt and The Medical Foundation.

Received: January 3, 2006
Revised: February 20, 2007
Accepted: April 25, 2007
Published online: June 28, 2007

REFERENCES

Berland, R., and Wortis, H.H. (2002). Origins and functions of B-1 cells with notes on the role of CD5. Annu. Rev. Immunol. *20*, 253–300.

Bikah, G., Carey, J., Ciallella, J.R., Tarakhovsky, A., and Bondada, S. (1996). CD5-mediated negative regulation of antigen receptor-induced growth signalings in B-1 B cells. Science *274*, 1906–1909.

Bolland, S., and Ravetch, J.V. (2000). Spontaneous autoimmune disease in FcgammaRIIB-deficient mice results from strain-specific epistasis. Immunity *13*, 277–285.

Bygrave, A.E., Rose, K.L., Cortes-Hermandez, J., Warren, J., Rogby, R.J., Cook, H.T., Walport, M.J., Vyse, T., and Botto, M. (2004). Spontaneous autoimmunity in 129 and C57BL/6 mice-implicatins for autoimmunity described in gene-targeted mice. PLoS Biol. *2*, 1081–1090.

Casola, S., Otipoby, K.L., Alimzhanov, M., Humme, S., Uyttersprot, N., Kutok, J.L., Carroll, M.C., and Rajewsky, K. (2004). B cell receptor signal strength determines B cell fate. Nat. Immunol. *5*, 317–327.

Cyster, J.G., and Goodnow, C.C. (1995). Protein tyrosine phosphatase 1C negatively regulates antigen receptor signaling in B lymphocytes and determines thresholds for negative selection. Immunity *2*, 13–24.

Förster, I., and Rajewsky, K. (1987). Expansion and functional activity of Ly-1$^+$ B cells upon transfer of peritoneal cells into allotype-congenic, newborn mice. Eur. J. Immunol. *17*, 521–528.

Gommerman, J.L., Oh, D.Y., Zhou, X., Tedder, T.F., Maurer, M., Galli, S.J., and Carroll, M.C. (2000). A role for CD21/35 and CD19 in responses to acute septic peritonitis: A potential mechanism for mast cell activation. J. Immunol. *165*, 6915–6921.

Gu, H., Förster, I., and Rajewsky, K. (1990). Sequence homologies, N sequence insertion and JH gene utilization in VHDJH joining: Implications for the joining mechanism and the ontogenetic timing of Ly1 B cell and B-CLL progenitor generation. EMBO J. *9*, 2133–2140.

Gu, H., Förster, I., and Rajewsky, K. (1992). Study of murine B-cell development through analysis of immunogloblin variable regions genes. Ann. N Y Acad. Sci. *651*, 304–310.

Guinamard, R., Okigaki, M., Schlessinger, J., and Ravetch, J.V. (2000). Absence of marginal zone B cells in Pyk-2 deficient mice defines their role in the humoral response. Nat. Immunol. *1*, 31–36.

Hardy, R.R., and Hayakawa, K. (2001). B cell development pathways. Annu. Rev. Immunol. *19*, 595–621.

Haughton, G., Arnold, L.W., Whitmore, A.C., and Clarke, S.H. (1993). B-1 cells are made, not born. Immunol. Today *14*, 84–87.

Hayashi, S.-I., Witte, P.L., Shultz, L.D., and Kincade, P.W. (1988). Lymphohemopoiesis in culture is prevented by interaction with adherent bone marrow cells from mutant viable motheaten mice. J. Immunol. *140*, 2139–2147.

Herzenberg, L.A., Stall, A.M., Lalor, P.A., Sidman, C., Moore, W.A., Parks, D., and Herzenberg, L.A. (1986). The Ly-1 B cell lineage. Immunol. Rev. *93*, 81–102.

Kantor, A.B., and Herzenberg, L.A. (1993). Origin of murine B cell lineages. Annu. Rev. Immunol. *11*, 501–538.

Kozolowski, M., Mlinaric-Rascan, I., Feng, G.S., Shen, R., Pawson, T., and Siminovitch, K.A. (1993). Expression and catalytic activity of the tyrosine phosphatase PTP1C is severely impaired in motheaten and viable motheaten mice. J. Exp. Med. *178*, 2157–2163.

Kühn, R., Schwenk, F., Aguet, M., and Rajewsky, K. (1995). Inducible gene targeting in mice. Science *269*, 1427–1429.

Lajaunias, F., Nitschke, L., Moll, T., Martinez-Soria, E., Semac, I., Chicheportiche, Y., Parkhouse, R.M.E., and Izui, S. (2002). Differentially regulated expression and function of CD22 in activated B-1 and B-2 lymphocytes. J. Immunol. *168*, 6078–6083.

Martin, A., Tsui, H.W., Shulman, M.J., Isenman, D., and Tsui, W.L. (1999). Murine SHP-1 splice variants with altered Src Homology 2 (SH2) domains. J. Biol. Chem. *274*, 21725–21734.

Medlock, E.S., Goldschneider, I., Greiner, D.L., and Shultz, L. (1987). Defective lymphopoisis in the bone marrow of motheaten (me/me) and viable motheaten (mev/mev) mutant mice. II. Description of a microenvironmental defect for the generation of terminal deoxynucleotidyltransferase-positive bone marrow cells in vitro. J. Immunol. *138*, 3590–3597.

Montecino-Rodriguez, E., Leathers, H., and Dorshkind, K. (2006). Identification of a B-1 B cell-specific progenitor. Nat. Immunol. *7*, 293–301.

Munn, D.H., Sharma, M.D., Hou, D., Baban, B., Lee, J.R., Antonia, S.J., Messina, J.L., Chandler, P., Koni, P., and Mellor, A.L. (2004). Expression of indoleamine 2,3-dioxygenase by plasmacytoid dendritic cells in tumor-draining lymph nodes. J. Clin. Invest. *114*, 280–290.

Neel, B.G., Hu, G., and Pao, L. (2003). The 'Shp'ing news: SH2 domain-containing tyrosine phosphatases in cell signaling. Trends Biochem. Sci. *28*, 284–293.

Nitschke, L., Carsetti, R., Ocker, B., Köhler, G., and Lamers, M.C. (1997). CD22 is a negative regulator of B-cell receptor signalling. Curr. Biol. *7*, 133–143.

O'Keefe, T.L., Williams, G.T., Batista, F.D., and Neuberger, M.S. (1999). Deficiency in CD22, a B cell-specific inhibitory receptor, is sufficient to predispose to development of high affinity autoantibodies. J. Exp. Med. *189*, 1307–1313.

O'Keefe, T.L., Williams, G.T., Davies, S.L., and Neuberger, M.S. (1996). Hyperresponsive B cells in CD22-deficient mice. Science *274*, 798–801.

Otipoby, K.L., Andersson, K.B., Draves, K.E., Klaus, S.J., Farr, A.G., Kerner, J.D., Permutter, R.M., Law, C.-L., and Clark, E.A. (1996). CD22 regulates thymus-independent responses and the lifespan of B cells. Nature *384*, 634–637.

Pan, C., Baumgarth, N., and Parnes, J.R. (1999). CD72-deficient mice reveal nonredundant roles of CD72 in B cell development and activation. Immunity *11*, 495–506.

Pani, G., Kozlowski, M., Cambier, J.C., Mills, G.B., and Siminovitch, K.A. (1995). Identification of the tyrosine phosphatase PTP1C as a B cell antigen receptor-associated protein involved in the regulation of B cell signaling. J. Exp. Med. *181*, 2077–2084.

Pritchard, N.R., and Smith, K.G.C. (2003). B cell inhibitory receptors and autoimmunity. Immunology *108*, 263–273.

Rickert, R.C., Roes, J., and Rajewsky, K. (1997). B lymphocyte-specific, Cre-mediated mutagenesis in mice. Nucleic Acids Res. *25*, 1317–1318.

Roes, J., and Rajwesky, K. (1993). Immunoglobulin D (IgD)-deficient mice reveal an auxiliary receptor function for IgD in antigen-mediated recruitment of B cells. J. Exp. Med. *177*, 45–55.

Sato, S., Miller, A.S., Inaoki, M., Bock, C.B., Jansen, P.J., Tang, M.L.K., and Tedder, T.F. (1996a). CD22 is both a positive and negative regulator of B lymphocyte antigen receptor signal transduction: Altered signaling in CD22-deficient mice. Immunity *5*, 552–602.

Sato, S., Ono, N., Steeber, D.A., Pisetsky, D.S., and Tedder, T.F. (1996b). CD19 regulates B lymphocyte signal thresholds critical for the development of B-1 lineage cells and autoimmunity. J. Immunol. *157*, 4371–4378.

Shultz, L.D. (1998). Pleiotrophic effects of deleterious alleles at the "motheaten" locus. Curr. Top. Microbiol. Immunol. *137*, 216–222.

Shultz, L.D., Schweitzer, P.A., Rajan, T.V., Yi, T., Ihle, J.N., Matthews, R.J., Thomas, M.L., and Beier, D.R. (1993). Mutations at the murine motheaten locus are within the hematopoietic cell protein-tyrosine phosphatase (Hcph) gene. Cell *73*, 1445–1454.

Sidman, C.L., Shultz, L.D., Hardy, R.R., Hayakawa, K., and Herzenberg, L.A. (1986). Production of immunoglobulin isotypes by Ly-1$^+$ B cells in viable motheaten and normal mice. Science *232*, 1423–1425.

Tsui, H.W., Siminovitch, K.A., de Souza, L., and Tsui, F.W. (1993). Motheaten and viable motheaten mice have mutations in the haematopoietic cell phosphatase gene. Nat. Genet. *4*, 124–129.

Ujike, A., Takeda, A., Nakamura, A., Ebihara, S., Akiyama, K., and Takai, T. (2002). Impaired dendritic cell maturation and increased T_H2 responses in PIR-B$^{-/-}$ mice. Nat. Immunol. *3*, 542–548.

Ye, M., Iwasaki, H., Laiosa, C.V., Stadtfeld, M., Xie, H., Heck, S., Clausen, B., Akashi, K., and Graf, T. (2003). Hematopoietic stem cells expressing the myeloid lysozyme gene retain long-term, multilineage repopulation potential. Immunity *19*, 689–699.

Yurasov, S., Wardemann, H., Hammersen, J., Tsuiji, M., Meffre, E., Pascual, V., and Nussenzweig, M.C. (2005). Defective B cell tolerance checkpoints in systemic lupus erythematosus. J. Exp. Med. *201*, 703–711.